

Structural, Magnetic, and Optical Properties of Co(II) in $\text{Co}_x\text{Cd}_{1-x}\text{In}_2\text{S}_4$ Spinel Solid Solutions

Piero Porta,¹ Anna Anichini,[†] and Maria Cristina Campa

Centro del Consiglio Nazionale delle Ricerche (CNR) su "Struttura e Attività Catalitica di Sistemi di Ossidi" (SACSO), Dipartimento di Chimica, Università La Sapienza, Piazzale Aldo Moro 5, 00185 Rome, Italy

Received December 23, 1993; in revised form April 15, 1994; accepted April 19, 1994

The cation distribution of several $\text{Co}_x\text{Cd}_{1-x}\text{In}_2\text{S}_4$ spinel solid solutions prepared in the solid state with different x values (0, 0.05, 0.1, 0.2, 0.4, 0.6, 0.8, and 1.0) has been studied by diffuse reflectance spectroscopy, magnetic susceptibility, lattice parameter variation, and analysis of some X-ray reflections whose intensities are particularly sensitive to variation in the cation positions. The results drawn from the combination of the four techniques indicate that Co^{2+} is present in both the octahedral and tetrahedral sites of the spinel structure and that the fraction of octahedral cobalt increases with the composition x , reaching the maximum value of 90% in CoIn_2S_4 . © 1995 Academic Press, Inc.

INTRODUCTION

The spinel structure is common to a wide class of inorganic compounds of considerable technological interest. Compounds belonging to the spinel group (mineral spinel composition is MgAl_2O_4) tend to have a chemical formula of the type XY_2Z_4 and a crystal structure based upon a face-centered cubic arrangement of anions Z with positions that are generally given by a parameter u according to the space group $Fd\bar{3}m$. The cations X and Y may have different valence states and may be distributed over the tetrahedral, T_d , and octahedral, O_h , interstitial sites of the anion lattice.

For a binary spinel containing divalent, X , and trivalent, Y , cations, two extreme distributions are possible: the "normal" $X[\text{Y}_2]\text{Z}_4$ and the "inverse" $Y[\text{XY}]\text{Z}_4$ ones (1), where the cations in the O_h sites (also called B sites, whereas the T_d sites are usually called A sites) are written in square brackets. Between these limiting cases intermediate distributions are possible, one being of particular interest, namely, the "random" $X_{1/3}Y_{2/3}[\text{X}_{2/3}Y_{4/3}]\text{Z}_4$ (2).

It is well known that the cation distribution in spinels, as well as in other inorganic compounds containing more than one coordination site, is determined by a fine balance

of several factors such as temperature and pressure, ion charge and radius, site preference energies, crystal and ligand field effects, anion polarization, and anion–anion repulsion effects (3–5). The possibility of forming solid solutions (ternary, quaternary, etc., compounds) adds one more variable, namely, the stoichiometric composition of the interchanging cations.

Studies of cation distribution in spinels are of considerable interest in solid state chemistry because they may allow an investigation of the relative stabilities of the metal ions in the T_d and O_h coordinations, and a better understanding of the correlation between structure and properties such as color, diffusivity, magnetic behavior, conductivity, catalytic activity, etc., which are well known to depend on the relative T_d and O_h occupancy by transition metal ions.

Several papers have been published on the work undertaken in our laboratory on oxidic spinel solid solutions (6). The field of interest was then extended to sulfide spinels with the aim of comparing the effect of a different anion on the cation distribution. It may be recalled that the sulfide framework is characterized by larger anions and a weaker crystal field, i.e., a larger delocalization and a larger covalent bond character, than the oxidic lattice.

EXPERIMENTAL

Preparation and chemical analysis. Polycrystalline samples of the general formula $\text{Co}_x\text{Cd}_{1-x}\text{In}_2\text{S}_4$ with $x = 0.0, 0.05, 0.1, 0.2, 0.4, 0.6, 0.8, \text{ and } 1.0$ were prepared by mixing stoichiometric quantities of the corresponding sulfides CoS , CdS , and In_2S_3 (pure materials from Cerac, Milwaukee, WI). To prevent oxidation the powders were pelleted, introduced into a silica tube, sealed under vacuum (about 10^{-4} mm Hg), and heated at 1173 K for 20 hr. The compounds showed colors varying from orange to black with the increase in cobalt content. The cobalt content, reported in Table I, was checked by atomic absorption.

¹ To whom correspondence should be addressed.

[†] Deceased. To whom this paper is dedicated.

TABLE 1
 $\text{Co}_x\text{Cd}_{1-x}\text{In}_2\text{S}_4$ Solid Solution Parameters

x_{nom}	x_{exp}	a	I_{400}/I_{220}	I_{400}/I_{422}	γ	μ_{exp}	μ_{XRD}	θ
0.00		10.8443	1.06	3.08				
0.05	0.05	10.8324	1.03	2.97	0.10	4.60	4.62	60
0.10	0.10	10.8278	1.01	2.91	0.20	4.65	4.68	70
0.20	0.19	10.8006	0.99	2.82	0.35	4.75	4.78	75
0.40	0.39	10.7516	0.94	2.72	0.49	4.85	4.86	85
0.60	0.58	10.6969	0.91	2.62	0.59	4.90	4.92	100
0.80	0.78	10.6453	0.88	2.47	0.70	4.96	4.97	125
1.00	1.00	10.5909	0.84	2.12	0.90	5.08	5.08	145

Note. Nominal, x_{nom} , and experimental, x_{exp} , cobalt content; lattice parameters, a (Å); experimental X-ray diffraction intensity ratios, I_{400}/I_{220} and I_{400}/I_{422} ; fraction of Co^{2+} ions in octahedral sites, γ ; experimental magnetic moments, $\mu_{\text{exp}}/\mu_{\text{B}}$; magnetic moments, $\mu_{\text{XRD}}/\mu_{\text{B}}$, calculated on the basis of the cobalt distribution by X-ray diffraction; Weiss constants, θ (K).

X-ray investigation and calculation of intensities. Iron-filtered $\text{CoK}\alpha$ radiation was used to investigate the compounds for both the lattice parameter and the intensity measurements. All samples showed very sharp reflections all having spinel cubic structure. For the determination of the lattice parameter a Debye camera (114.6 mm in diameter) was used with the asymmetric Straumanis film mounting method. During the exposure (8 hr) the camera temperature was observed to vary within 1–3 K. The values of a referred to 294 K and with an error evaluated to about 1×10^{-4} Å are reported in Table 1. The integrated intensities of the 400, 220, and 422 reflections were measured by the pulse counting method using a Philips high-angle goniometer spectrometer with a flat plate sample holder and a scanning rate of 0.25° per minute. All the specimens were run twice and after correction for the background a mean value of the intensities was taken. The mean value of the I_{400}/I_{220} and I_{400}/I_{422} observed intensity ratios are summarized in Table 1. It should be noted that the above-mentioned reflections and their relative intensity ratios were selected since they provide the best basis for determining the cation distribution in the spinel systems (7). The selection criteria for the given reflections and the calculation method for the relative intensities were the same as those adopted in previous works on the cation distribution of oxidic spinel solid solutions (6). The intensities were computed with a UNIVAC 1108 computer at Rome University with the following input data incorporated into the program: (i) the molar composition of the spinel; (ii) the value of the anion parameter, u , taken as constant (0.386) for all solid solutions since the CdIn_2S_4 and CoIn_2S_4 end members both have the previous value (5, 8, 10); (iii) the scattering factors for Co^{2+} , Cd^{2+} , In^{3+} , and S^{2-} ; and (iv) the Lorentz-polarization correction. No temperature correction was deemed necessary in the in-

tensity calculation since the spinels are high melting temperature compounds and the thermal vibration of the atoms at room temperature should have a negligible effect.

Magnetic susceptibility. The magnetic susceptibilities were measured using the Gouy method over the temperature range 100–295 K. Corrections were made for the diamagnetism of the samples; the susceptibilities were independent of the magnetic field strength. All materials follow Curie–Weiss behavior. The value of the Curie constant, C , and of the magnetic moment, μ , were taken for all specimens from the slopes of $1/\chi_{\text{at}}$ vs T plots. The values of the Weiss temperature, θ , in the Curie–Weiss expression $\chi_{\text{at}} = C/(T + \theta)$ were taken from the intercepts of the $1/\chi_{\text{at}}$ lines on the T axis.

Reflectance spectroscopy. Reflectance spectra in the wavelength range 2500–400 nm ($4000\text{--}25,000\text{ cm}^{-1}$) were recorded on a Beckman DK-1 spectrometer with a standard reflectance attachment against pure CdIn_2S_4 as reference.

RESULTS AND DISCUSSION

Pure CdIn_2S_4 and CoIn_2S_4 are referred to as “normal” and nearly “inverse” spinels, respectively (5, 8, 10). In the former compound the Cd^{2+} and In^{3+} ions occupy the tetrahedral (T_d) and octahedral (O_h) sites of the spinel structure, respectively; in CoIn_2S_4 , most of the Co^{2+} ions are in O_h symmetry, and In^{3+} is distributed between the O_h and T_d sites.

As shown by Bertaut (7), the comparison between experimental and calculated results for two different and most diagnostic intensity ratios of XRD reflections, namely the I_{400}/I_{220} and I_{400}/I_{422} ones, is in general sufficient to determine the cation distribution in the spinel structure. Due to the “normality” of CdIn_2S_4 and to the strong preference for tetrahedral coordination of the Cd^{2+} ions (9), our study for the $\text{Co}_x\text{Cd}_{1-x}\text{In}_2\text{S}_4$ solid solutions was restricted to find the interchange of the site symmetry of Co^{2+} and In^{3+} in function of the compositional parameter x .

The values found for the fraction of Co^{2+} in the octahedral sites, γ , are reported in Table 1 and shown in Fig. 1. The results show that there is a continuous increase in octahedral cobalt occupation at the augmenting of x . Pure CoIn_2S_4 results 90% “inverse.”

Another method of examining changes in the coordination of paramagnetic ions, such as Co^{2+} in the $\text{Co}_x\text{Cd}_{1-x}\text{In}_2\text{S}_4$ solid solutions, is magnetic susceptibility. In fact for Co^{2+} in a tetrahedral field (high-spin $3d^7$ configuration, ground state 4A_2) the effective magnetic moment $\mu = \mu_{\text{SO}}$ ($1\text{--}4 \lambda/10\text{ Dq}$), where λ is the spin–orbit coupling constant, Dq is the crystal field strength and μ_{SO} is the spin-only value of the magnetic moment [for Co^{2+} $\mu_{\text{SO}} = 3.9 \mu_{\text{B}}$ (11)]. The experimental value of μ for Co^{2+} ions

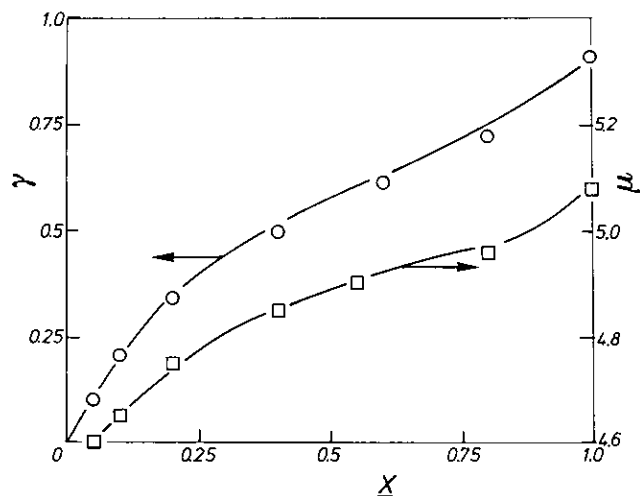


FIG. 1. Octahedral cobalt cation distribution γ (on the left) and experimental magnetic moments μ (on the right) vs cobalt content x .

in the T_d configuration is $4.55 \mu_B$, as found in CoRh_2O_4 (6e). For high-spin octahedral Co^{2+} ions the ground level (${}^4T_{1g}$) is orbitally degenerate and there is an appreciable orbital contribution to the magnetic moment (11). Experiments performed on $\text{Co}_x\text{Mg}_{1-x}\text{O}$ solid solutions have shown that $\mu = 5.25 \mu_B$ for Co^{2+} in the O_h configuration (12).

The results of the magnetic measurements are presented in Table 1; the values of the magnetic moments are also shown in Fig. 1. The experimental $1/\chi_{\text{at}}$ vs T plots for the samples with $x = 0.1, 0.4,$ and 0.8 (given as examples) together with the theoretically expected $1/\chi_{\text{at}}$ vs T plots for spin-only approximation (curve A), tetrahedral Co^{2+} (curve B), and octahedral Co^{2+} (curve C) are shown in Fig. 2. The complete set of results show that

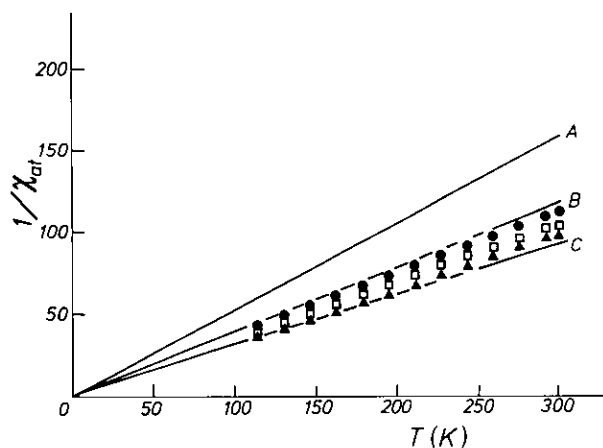


FIG. 2. Inverse atomic susceptibility $1/\chi_{\text{at}}$ vs temperature T for $\text{Co}_x\text{Cd}_{1-x}\text{In}_2\text{S}_4$ samples. Experimental: (●) $x = 0.1$; (□) $x = 0.4$; (▲) $x = 0.8$. Theoretical curves for Co^{2+} : (A) spin-only approximation; (B) tetrahedral symmetry; (C) octahedral symmetry.

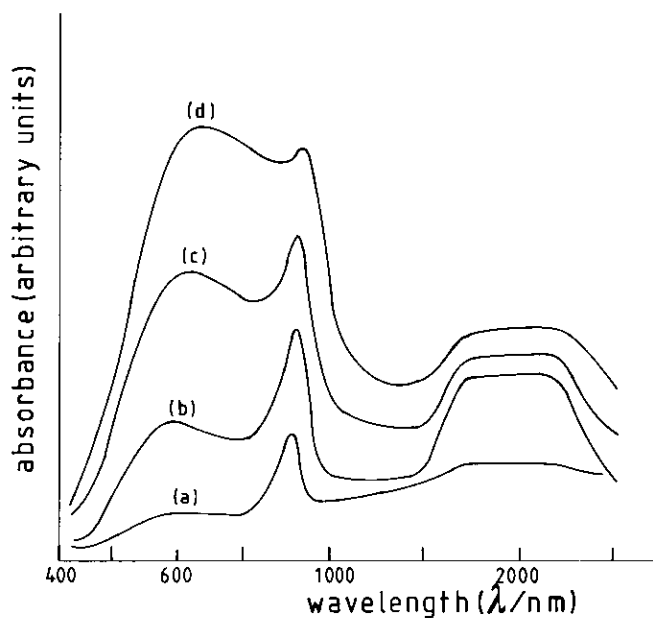


FIG. 3. Reflectance spectra for $\text{Co}_x\text{Cd}_{1-x}\text{In}_2\text{S}_4$ samples; (a) $x = 0.1$; (b) $x = 0.2$; (c) $x = 0.6$; (d) $x = 1.0$.

the magnetic values are all in the expected [by theory and experiment (11–15)] range for a cobalt distribution intermediate between T_d and O_h symmetry. Note that, with increasing cobalt content, the μ values increase; this behavior confirms the XRD results which have shown that the spinels become more and more inverse at the increase of x . Table 1 reports the magnetic moments, μ_{XRD} , calculated on the basis of the cobalt distribution found from X-ray diffraction and taking into account the values of μ for completely T_d and O_h cobalt occupation as 4.55 (6e) and 5.25 (12) μ_B , respectively. The agreement between experimental and calculated values is satisfactory. The values of the Weiss constant θ (derived from the intercepts with the T axis of the $1/\chi_{\text{at}}$ vs T plots and indicative of cobalt O_h – O_h antiferromagnetic interactions (13) increase with increasing cobalt content and so confirm the continuous increase of octahedral cobalt occupation.

Reflectance spectra are another tool for detecting octahedrally and tetrahedrally coordinated cobalt ions in solids (11). Figure 3 shows, for example, the DR spectra for the samples where $x = 0.1, 0.2, 0.6,$ and 1.0 . The following bands are visible: (i) a broad band in the region 2200 – 1500 nm (4500 – 6700 cm^{-1}); (ii) a peak at 880 nm (ca. $11,400$ cm^{-1}); (iii) a shoulder at 805 nm (ca. $12,400$ cm^{-1}); and (iv) a band at 590 nm (ca. $17,000$ cm^{-1}). Band (i) is due to both octahedral and tetrahedral Co^{2+} and it is an envelope of the unresolved bands corresponding to the tetrahedral ${}^4A_2(F) \rightarrow {}^4T_2(F)$ and ${}^4A_2(F) \rightarrow {}^4T_1(F)$ transition and to the octahedral ${}^4T_{1g}(F) \rightarrow {}^4T_{2g}(F)$ transition. Band (ii) corresponds to the tetrahedral spin-forbidden ${}^4A_2(F) \rightarrow$

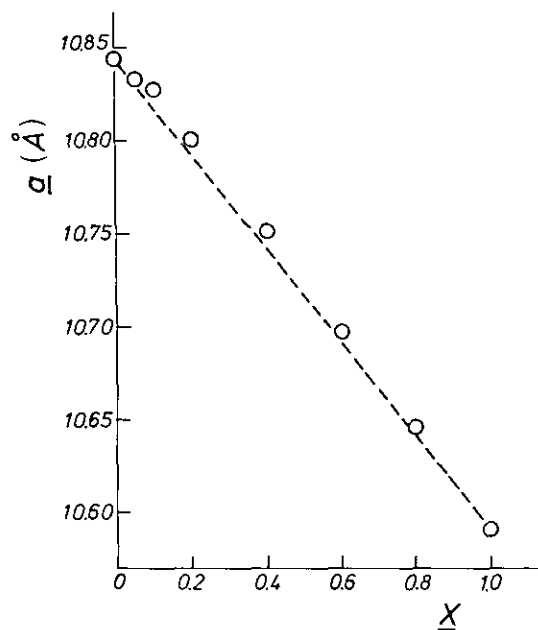


FIG. 4. Lattice parameter a (Å) vs cobalt content x for $\text{Co}_x\text{Cd}_{1-x}\text{In}_2\text{S}_4$ samples. The dashed line represents Vegard's law.

${}^2E(G)$ transition. The shoulder at $12,400\text{ cm}^{-1}$ can be attributed either to the tetrahedral ${}^4A_2(F) \rightarrow {}^4T_1(P)$ or to the octahedral ${}^4T_{1g}(F) \rightarrow {}^4A_{2g}(F)$ transitions. Band (iv) corresponds to the octahedral ${}^4T_{1g}(F) \rightarrow {}^4T_{1g}(P)$ transition. It may be observed from Fig. 3 that the intensity of the peak at $11,400\text{ cm}^{-1}$ (T_d symmetry) decreases, whereas the intensity of the band at $17,000\text{ cm}^{-1}$ (O_h symmetry) increases with increasing cobalt content. These findings agree with both XRD and magnetic results.

The decrease in the lattice parameter a (the data are presented in Table 1 and in Fig. 4) by going from CdIn_2S_4 (10.844 Å) to CoIn_2S_4 (10.591 Å) is explained in terms of substitution in the spinel lattice of larger Cd^{2+} ions [T_d ionic radius for Cd^{2+} equal to 0.78 Å (16)] with smaller Co^{2+} ions [T_d and O_h ionic radii for Co^{2+} equal to 0.58 and 0.75 Å , respectively (16)]. Note that our values of a for the CdIn_2S_4 and CoIn_2S_4 end members are in good agreement with those reported in the literature, 10.797 Å for CdIn_2S_4 (10), and 10.58 Å for CoIn_2S_4 (13).

It may be pointed out that, as shown in Figs. 1 and 4, the variations of lattice parameters, octahedral Co distribution, and magnetic moments versus cobalt content are not linear. These findings may indicate that different steps in T_d and O_h occupancies could be imagined within the solid solution formation.

It may finally be noted that the preferential octahedral

or tetrahedral site occupancy for transition elements as a function of the composition has also been recently discussed for the ternary $\text{In}_2\text{S}_3\text{-FeS-FeS}_2$ (17) and $\text{In}_2\text{S}_3\text{-Cu}_2\text{S-CuS}$ (18) systems.

CONCLUSIONS

By means of several complementary techniques the following points have been evidenced:

- (i) both tetrahedral and octahedral sites of the spinel structure are occupied by Co^{2+} ions;
- (ii) the amount of Co^{2+} in the octahedral sites increases with the increase of cobalt content and reaches the value of 90% in pure CoIn_2S_4 ; and
- (iii) as the octahedral cobalt occupation increases the antiferromagnetic interactions become stronger.

ACKNOWLEDGMENTS

We thank Mr. G. Minelli for technical assistance and Mr. M. Inversi for the drawings.

REFERENCES

1. T. F. Barth and E. Posnjak, *Z. Kristallogr.* **82**, 325 (1932).
2. F. Machatschki, *Z. Kristallogr.* **82**, 348 (1932).
3. J. Smit, F. K. Lotgering, and R. P. van Staplele, *J. Phys. Soc. Jpn.* **17**, B-1, 268 (1962).
4. H. Schmalzried, *Z. Phys. Chem. Neue Folge* **28**, 203 (1961).
5. G. Blasse, *Philips Res. Rep. Suppl.* No. 3, (1964).
6. (a) P. Porta, F. S. Stone, and R. G. Turner, *J. Solid State Chem.* **11**, 135 (1974); (b) P. Porta, A. Anichini, and U. Bucciarelli, *J. Chem. Soc. Faraday Trans 1* **73**, 1972 (1977); (c) P. Porta and A. Anichini, *J. Chem. Soc. Faraday Trans 1* **76**, 2448 (1980); (d) P. Porta and A. Anichini, *Z. Phys. Chem. Neue Folge* **127**, 223 (1981); (e) P. Porta, A. Anichini, and A. Guglietti, *Gazz. Chim. Ital.* **113**, 595 (1983).
7. E. F. Bertaut, *Compt. Rend.* **230**, 213 (1950).
8. H. Hahn and W. Klinger, *Z. Anorg. Allg. Chem.* **263**, 177 (1950).
9. J. D. Dunitz and L. E. Orgel, *J. Phys. Chem. Solids* **3**, 20 (1957).
10. R. J. Hill, J. R. Craig, and G. V. Gibbs, *Phys. Chem. Miner.* **4**, 317 (1979).
11. B. N. Figgis, "Introduction to Ligand Field." Wiley, New York, 1966.
12. A. Cimino, M. Lo Jacono, P. Porta, and M. Valigi, *Z. Phys. Chem. Neue Folge* **70**, 166 (1970).
13. S. Schlein, Thesis, Brown University, Providence, RI, 1971; Univ. Microfilms, Ann Arbor, MI.
14. M. M. Schieber, "Experimental Magnetochemistry." North-Holland, Amsterdam, 1967.
15. P. Porta and A. Anichini, *J. Chem. Soc., Faraday Trans 1* **76**, 2448 (1980).
16. R. D. Shannon, *Acta Crystallogr. Sect. A* **32**, 751 (1976).
17. M. Womes, J. Olivier-Fourcade, J. C. Jumas, F. Aubertin, and U. Gonser, *J. Solid State Chem.* **97**, 249 (1992).
18. F. Py, J. Olivier-Fourcade, and J. C. Jumas, *J. Solid State Chem.* **97**, 319 (1992).